Proc. Int. Symposium on Neutron Optics and Related Research Facilities, Kumatori, 1996
J. Phys. Soc. Jpn. **65** (1996) Suppl. A pp. 199-202

Polarizing Beam-Splitter Device at a Pulsed Neutron Source

Shinichi Itoh and *Masayasu Takeda

Booster Synchrotron Utilization Facility, National Laboratory for High Energy Physics, Tsukuba 305, Japan
**Department of Physics, Tohoku University, Sendai 980-77, Japan*

(Received 23 January 1996; accepted 15 June 1996)

A polarizing beam-splitter device was designed using Fe/Si supermirrors in order to obtain two polarized neutron beam lines, from one unpolarized neutron beam line, with a practical beam size for investigating the properties of condensed matter. This device was mounted after a guide tube at a pulsed neutron source, and its performance was investigated.

KEYWORDS: neutron polarizer, beam splitter, supermirror, pulsed neutron source

§.1. Introduction

A recent increase in the critical wavenumber of supermirrors has contributed to the improvement of polarizers at a pulsed neutron source, where a wide wavelength band is required. The principle of supermirror polarizers is to use magnetized multi-bilayers with slowly varying d-spacings, which produce a superpositioning of Bragg reflections over a range of wavelengths (λ) from λ_{min} to λ_{max}. The combination of materials for the magnetic and nonmagnetic layers is chosen so that the difference between the nuclear and magnetic scattering-length densities of the magnetic material can be made equal to the nuclear scattering-length density of the nonmagnetic material, and eventually neutrons in one spin state are reflected by the supermirror and those in the other state are transmitted. The minimum wavelength (λ_{min}) is determined by the minimum d-spacing. A supermirror is characterized by the critical wavenumber (Q_c) corresponding to the minimum d-spacing and Q_c is normally represented in units of the critical wavenumber of the total reflection from natural nickel, Q_c^{Ni}. On the other hand, for an Fe/Si supermirror evaporated onto a silicon substrate,[1] for instance, λ_max is limited to the total reflection from the substrate; at $\lambda>\lambda_{max}$, total reflection occurs for neutrons in both spin states. The critical wavenumber of the total reflection from the substrate is normally half that of Q_c^{Ni}. Recently, since supermirrors with $Q_c \sim 3\, Q_c^{Ni}$ have become commercially available, polarized beams can be obtained over a wider wavelength band accessible at a pulsed cold neutron source.

It is necessary to install as many spectrometers as possible at a neutron scattering facility having a limited number of beam holes. At a steady neutron source, since most spectrometers use a monochromatic beam, many neutron beam lines can easily be made to branch from one beam line by using the Bragg reflection from a crystal. At a pulsed neutron source, however, the Bragg reflection from a crystal is not suitable for a beam branch, because each spectrometer requires a wide wavelength band, and, therefore, a device using a supermirror is a possible candidate to satisfy such a requirement. The beam separation with twice the angle of the grazing angle of the supermirror is obtained in such a device as the transmitted beam as well as reflected beam from the supermirror is used.[2] We designed a polarizing beam-splitter device based on the above concept in order to obtain two polarized neutron beam lines with a practical beam size suitable for investigating the properties of condensed matter from one unpolarized neutron beam line. The polarizing beam-splitter device was mounted after a guide tube at a pulsed cold-neutron source, and its performance was investigated.

§.2. Experimental set-up

The polarizing beam-splitter device (manufactured by Osmic Inc.) has a trapezoidal shape from the top view; supermirrors were mounted on the line between the apex and the middle point of the opposite side, as shown in Fig.1. The outlet area is twice that of the inlet area (1.8cm × 5cm (width × height)). Half of the outlet area is for the transmitted beam through the supermirrors; the other half is for the reflected beam. We chose Fe/Si supermirrors evaporated onto a silicon substrate[1] because less neutron absorption from the substrate is suitable for the transmitted beam. Since Q_c of the supermirrors used in the present device was 0.064Å^{-1} (mentioned below), the supermirrors were mounted by keeping a grazing angle of $\theta_0 = 0.9°$ for the incoming neutrons to the supermirrors in the present device in order to obtain a polarized neutron beam at

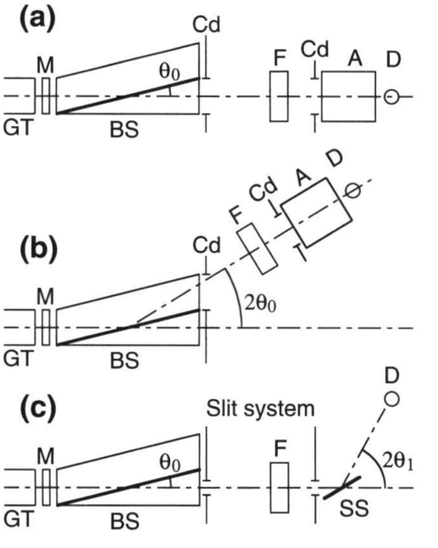

Fig. 1. Schematic drawing of the experimental set-up for a measurement of the transmitted beam (a) that of the reflected beam (b) and the sample supermirror measurement (c). GT, M, BS, Cd, F, A, SS and D denote the guide tube, monitor, polarizing beam-splitter device, cadmium mask, spin flipper, spin analyzer, sample supermirror and detector, respectively.

$\lambda > 3$Å; eventually, the length of the device became 118 cm including flanges. The supermirrors were assembled in a boron-glass tube and the inside walls of the tube were coated with natural nickel. A boron-glass tube was mounted in a magnetic housing to apply a magnetic field of 300 Oe to the supermirrors. The present device was mounted after a guide tube (natural nickel coating) of the C3 cold-neutron beam hole[3] at the pulsed neutron source (KENS) at National Laboratory for High Energy Physics; a schematic drawing of the experimental set-up is shown in Fig.1.

For measuring the transmitted beam, a spin flipper and a spin analyzer were mounted on the beam line of the transmission direction, as shown in Fig.1 (a). The spin flipper was a $1/t$ flipper, which generates a magnetic field that is inversely proportional to the time of flight of neutrons, synchronized with the repetition of the pulsed neutron source; therefore, a λ-independent flipping efficiency was obtained. The spin analyzer was a Soller slit comprising Co/Ti supermirrors.[4] For measuring the transmitted beam, the outlet area for the reflected beam was masked with a cadmium plate. As shown in Fig.1(b), the measurement of the reflected beam, the spin flipper and the spin analyzer were mounted along the reflection direction, and the transmitted beam was masked. In these experimental set-ups, since the beam was collimated by the geometrical structure of the present device, the geometrically-determined beam divergence (geometrical collimation) was $\Delta\theta_0 = 0.9°$. The incident beam extracted from the guide tube has a λ-dependent beam divergence, $\Delta\theta_i/\lambda$ = 0.099 deg/Å(= $Q_c^{\mathrm{Ni}}/4\pi$), as a result of the total reflection on the nickel surface. The smaller quantity in $\Delta\theta_i$ and $\Delta\theta_0$ is effective for the performance of the present device.

Furthermore, in order to characterize the supermirror used in the present device, the reflectivity measurement shown in Fig.1(c) was performed. Instead of the spin analyzer, an Fe/Si supermirror sample, which was evaporated under the same condition as that for the supermirrors used in the present device, was mounted in a magnetic field of 9.6 kOe. The neutron beam was collimated with a slit system, which determined the geometrical collimation to be $\Delta\theta_0$ = 0.057°. The reflectivity was obtained from the ratio of the reflected intensity from the sample supermirror against the intensity measured without the sample supermirror at the direct beam position.

§.3. Supermirror

The supermirror used in the polarizing beam-splitter device was evaporated onto a single-crystal silicon substrate with a thickness of 0.6 mm. The same coating as that of the supermirror structure was performed on both sides of the silicon substrate in order to improve the flatness of the supermirror.[5] When the supermirror structure was coated on a single side, the flatness (deviation of the surface) was 0.4°; on the other hand, the flatness of the original substrate (less than 0.02°) was almost maintained by coating both sides.[5] Since a flatness of 0.4° was not appropriate for the present device, where the grazing angle was 0.9°, coating both sides was chosen

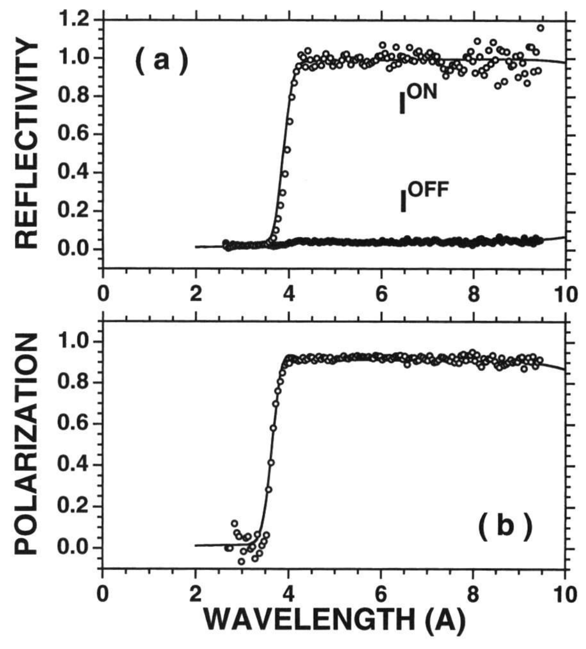

Fig. 2. Observed spin-dependent reflectivity (a) and polarization (b) of the sample Fe/Si supermirror. The solid lines are calculations based on the thickness distribution of the supermirror.

in the present manufacturing. For reflectivity measurement, as shown in Fig.1 (c), a single-side coated supermirror was used for the sample supermirror, because the flatness could be recovered at the sample mounting.

The wavenumber (Q) dependence of the reflectivities of the supermirror ($R^+(Q)$ and $R^-(Q)$) for up-spin and down-spin, respectively, can be calculated[6] from the thickness distribution of the supermirror.[5] In the critical region, the wavenumber where the reflectivity drops to 0.95 was calculated to be 0.064Å^{-1} and 0.0117Å^{-1} for $R^+(Q)$ and $R^-(Q)$, respectively. The wavenumber of 0.064Å^{-1} is almost $3Q_c^{\mathrm{Ni}}$. The critical wavelengths of the present device ($\lambda_c^{\pm}$) are converted from the critical wavenumbers for up-spin and down-spin by using the grazing angle. Due to the thickness distribution,[5] $R^+(Q)$ showed a dip (decrease of reflectivity) at around Q = 0.022Å^{-1}. In the calculation, since interdiffusions between the layers were neglected, $R^+(Q) = 1$ at $Q < Q_c$, except at the above-mentioned dip.

The observed polarization ($P_{\mathrm{OBS}}(\lambda)$) and reflectivities ($I_{\mathrm{OBS}}^{\mathrm{ON}}(\lambda)$ and $I_{\mathrm{OBS}}^{\mathrm{OFF}}(\lambda)$) of the sample supermirror are shown in Fig.2. The superscript of the reflectivity represents the state of the spin flipper. The polarization can be obtained from the reflectivities through the following relation, where the flipping efficiency is 1:

$$P_{\mathrm{OBS}}(\lambda) = \frac{I_{\mathrm{OBS}}^{\mathrm{ON}}(\lambda) - I_{\mathrm{OBS}}^{\mathrm{OFF}}(\lambda)}{I_{\mathrm{OBS}}^{\mathrm{ON}}(\lambda) + I_{\mathrm{OBS}}^{\mathrm{OFF}}(\lambda)} \qquad (1)$$

Although the relative values of the reflectivities were experimentally obtained, the proportional constant to the reflectivities was canceled for deducing the polarization, as shown in the above equation. The reflectivity data were scaled to the calculations. We calculate the λ-dependent reflectivities ($I^{\pm}(\theta,\lambda)$) at a fixed grazing angle (θ) with the actual beam collimation, from $R^{\pm}(Q)$, and the following polarizations were calculated;

$$P_0(\lambda)=\frac{(1-I^-(\theta_0,\lambda))-(1-I^+(\theta_0,\lambda))}{(1-I^-(\theta_0,\lambda))+(1-I^+(\theta_0,\lambda))}, \quad (2)$$

$$P_1(\lambda)=\frac{I^+(\theta_1,\lambda)-I^-(\theta_1,\lambda)}{I^+(\theta_1,\lambda)+I^-(\theta_1,\lambda)}, \quad (3)$$

where θ_0 and θ_1 are the grazing angles of the supermirror in the present device and that of the sample supermirror, respectively. $P_0(\lambda)$ is the polarization of the beam transmitted through the supermirror in the present device, $P_1(\lambda)$ is that of the reflected beam from the sample supermirror and the observation is compared with $P(\lambda) = P_0(\lambda)P_1(\lambda)$. The reflectivities corresponding to the experimental condition are calculated as follows:

$$I^{\mathrm{ON}}(\lambda)=P_0^+(\lambda)I^+(\theta_1,\lambda)+P_0^-(\lambda)I^-(\theta_1,\lambda) \quad (4)$$

$$I^{\mathrm{OFF}}(\lambda)=P_0^-(\lambda)I^+(\theta_1,\lambda)+P_0^+(\lambda)I^-(\theta_1,\lambda) \quad (5)$$

where $P_0^{\pm}(\lambda)=(1\pm P_0(\lambda))/2$. The observed quantities were well described by a calculation with $\theta_0 = 1.07°$ and $\theta_1 = 1.16°$, as shown in Fig.2. In other words, the observed behavior is consistent with a calculation using only the thickness distribution without any interdiffusion between layers. The critical wavelength in the polarization comes from θ_0 and that in the reflectivity from θ_1. The polarization at $\lambda > \lambda_c^+$ was 0.92, where $P_0(\lambda)$ and $P_1(\lambda)$ were calculated to be 1.00 and 0.92, respectively. The polarization of the reflected beam ($P_1(\lambda)$) is determined by the layer structure with the contrast; on the other hand, $P_0(\lambda) = 1$ if $R_+(Q) = 1$, as shown in eq.(2).

§.4. Polarizing beam-splitter device

We now discuss the performance of the polarizing beam-splitter device measured in the experimental set-up shown in Figs.1 (a) and (b). The quantities which describe the performance are listed with the calculation formulae as follows:

$$P_T(\lambda)=\frac{(1-I^-(\theta_0,\lambda))-(1-I^+(\theta_0,\lambda))}{(1-I^-(\theta_0,\lambda))+(1-I^+(\theta_0,\lambda))}, \quad (6)$$

$$P_R(\lambda)=\frac{I^+(\theta_1,\lambda)-I^-(\theta_1,\lambda)}{I^+(\theta_1,\lambda)+I^-(\theta_1,\lambda)}, \quad (7)$$

$$I_T(\lambda)=e^{-n\sigma t/\sin\theta_0}(2-I^-(\theta_0,\lambda)-I^+(\theta_0,\lambda)), \quad (8)$$

$$I_R(\lambda)=I^+(\theta_0,\lambda)+I^-(\theta_0,\lambda), \quad (9)$$

where "P" and "I" denote the polarization and intensity (sum of the intensities of both spin states); the subscripts "T" and "R" denote the transmitted and reflected beams, respectively. The exponential factor in eq.(8) is the intensity loss due to absorption through the silicon substrate, calculated from the number density (n=5.00×10^{22} cm^{-3}), the λ-dependent total cross section (σ)[7] and the thickness (t = 0.6mm). The λ-dependent

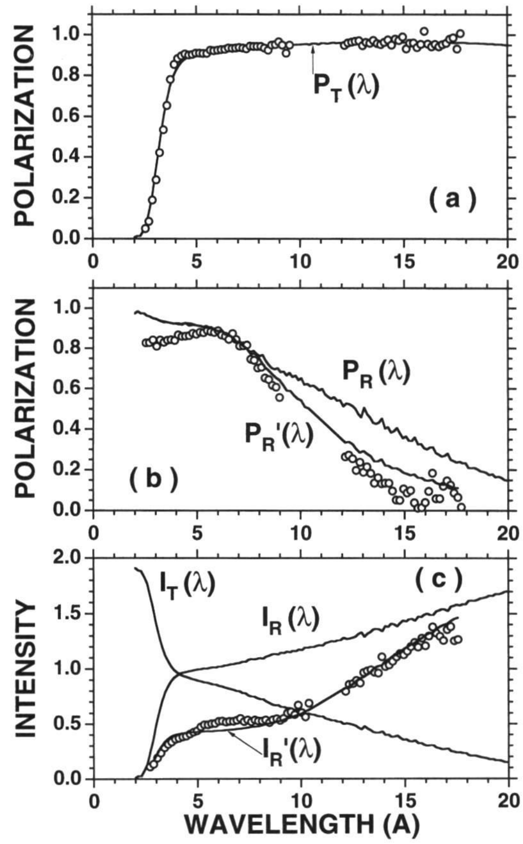

Fig. 3. Performance of the polarizing beam-splitter device. The marks are the observed data of the polarization of the transmitted beam (a), the polarization of the reflected beam (b) and the intensity of the reflected beam (c); the solid lines are the calculations. $P_T(\lambda)$, $P_R(\lambda)$, $I_T(\lambda)$ and $I_R(\lambda)$ were calculated based on the reflectivity of the supermirror; $P_{R'}(\lambda)$ and $I_{R'}(\lambda)$ include the attenuation of the intensity and the contamination of the unpolarized neutrons for the reflected beam.

reflectivities ($I^{\pm}(\theta_0,\lambda)$) in the actual beam collimation were calculated from the supermirror reflectivities (described below). Figure 3 shows these calculated quantities along with the experimental results. Since up-spin neutrons are reflected at $\lambda > \lambda_c^+$, the main component of the transmitted beam is the down-spin neutrons and that of the reflected beam the up-spin neutrons. The polarization of the transmitted beam ($P_T(\lambda)$) increases with λ and $P_T(\lambda) = 1$ at $\lambda > \lambda_c^+$ if $I^+(\theta_0,\lambda)$=1. At $\lambda < \lambda_c^+$, $I_T(\lambda)$ is greater than 1 due to the transmission of down-spin neutrons, where the intensity of the incident unpolarized beam is defined to be 2. At $\lambda = \lambda_c^+$, $I_R(\lambda)$ increases due to the reflection of up-spin neutrons and becomes greater than 1 at larger λ due to the reflection of the down-spin neutrons. At $\lambda > \lambda_c^-$, $I_R(\lambda)$ should be 2 because of the total reflection of neutrons in both spin states; however, the critical region of the down-spin reflectivity is smeared out due to the large beam divergence, and eventually the intensity gradually increases. The experimental data shown in Fig.3 were obtained by correcting the polarizing efficiency of the spin analyzer and the flipping efficiency of the spin flipper for the observed polarizations. The λ dependence of the polarizing efficiency of the spin analyzer is described by an empirical formula established by another measurement, and the flipping efficiency was presently determined to be

1.0 for $\lambda < 10$Å and 0.8 for $\lambda > 10$Å by a measurement of a shim plate.

The polarization of the transmitted beam can be calculated using eq.(6) with the actual beam collimation. In the experimental set-up shown in Figs.1(a) and (b), since the intensity of the transmitted beam was maximized, the grazing angle of the supermirrors in the present device should be θ_0 = 0.9°; in fact, λ_c^+ is consistent with a calculation with θ_0 = 0.9° (in the supermirror sample set-up, the beam axis was slightly different from that in this optimization). First, by using the above-mentioned $R^{\pm}(Q)$ calculated from only the thickness distribution, $P_T(\lambda)$ was calculated to be 1 at $\lambda > \lambda_c^+$, contrary to the observed polarization less than 1. As mentioned above, $P_T(\lambda)=1$ results from $R^+(Q)=1$. Therefore, we introduced the factor, $\alpha(Q)$, to reproduce the actual reflectivity, and calculated the polarization in eq.(6) using $\alpha(Q)R^{\pm}(Q)$ instead of $R^{\pm}(Q)$, where a monotonous empirical formula for $\alpha(Q)$ was established on the assumption that $\alpha(Q)$ = 1, 0.99, 0.95 and 0.93 at Q = 0, 0.02, 0.04 and 0.06Å^{-1}, respectively. This Q-dependent factor is consistent with a nominal specification of the reflectivity of a $3Q_c^{\mathrm{Ni}}$ supermirror.[5] As shown in Fig.3(a), the observed polarization was well described by the calculation.

On the other hand, as shown in Figs. 3(b) and (c), the observed polarization and intensity of the reflected beam was much less than the calculation. The observed spectrum was comparable to the quantity in eq.(8) or (9) multiplied by the incident-beam spectrum ($I_i(\lambda)$). Since the polarization of the transmitted beam was well described by the calculation, assuming the observed spectrum of the transmitted beam to be $I_i(\lambda)I_T(\lambda)$, the incident-beam spectrum can be deduced by using the calculated value of $I_T(\lambda)$. The observed intensity of the reflected beam shown in Fig.3(c) was obtained by using $I_i(\lambda)$ deduced from the transmitted beam spectrum. The less intensity and less polarization result from the more divergent beam of the reflected neutrons and the existence of unpolarized neutrons coming to the spin analyzer without reflecting on the supermirror, respectively. In fact, the following intensity greatly improved the calculation describing the observed intensity:

$$I'_R(\lambda) = AI_R(\lambda) + \frac{B}{\Delta\theta_i(\lambda)}\exp\left(-\frac{(4\ln 2)\theta^2}{\Delta\theta_i(\lambda)^2}\right), \tag{10}$$

where the first term is the attenuation of the intensity and the second term is the contamination of unpolarized neutrons. In the first term, the geometrically-obtained attenuation factor, $A=(w_1/L_1)/(w_0/L_0)$, was used, where w_0 = 1.8 cm and L_0 = 59cm are the outlet area and the half length of the present device, respectively, w_1 = 2.0cm is the aperture of the spin analyzer, and L_1 = 203 cm is the distance between the center of the present device and the inlet of the spin analyzer. The second term is the beam spread of the incident neutrons through the guide tube, detected at the spin-analyzer direction of θ=1.2°. The factor, B, is an adjustable parameter and $\Delta\theta_i(\lambda)$ is the λ-dependent incident beam divergence mentioned in Sec.2. The calculated polarization, $P_R'(\lambda)$, corresponding to eq.(10) greatly improved the calculation describing the observed polarization shown in Fig.3(b).

§.5. Summary

We demonstrated an investigation of the performance of the polarizing beam-splitter device installed at a pulsed cold-neutron source. The result of a reflectivity measurement of the sample supermirror shows that the supermirrors in the present device were made with good quality: a clear critical region and high reflectivity. Moreover, the polarization of the transmitted beam from the present device also shows that the reflectivity of the supermirrors was high, even at Q_c. The performance of the transmitted beam through the present device was well explained by a model calculation. Although that of the reflected beam was less than the model calculation, the performance could be understood using the geometrical configuration of the experimental set-up: the reflected beam was more divergent and contaminated by unpolarized neutrons. The present device is more optimized for the transmitted beam and the transmitted beam is suitable for polarization-required or collimation-controlled experiments. Although the reflected beam is more divergent and less polarized, it is more intense than the transmitted beam, therefore, the reflected beam is suitable for intensity-required experiments if a device by which the neutron beam can be converged is placed just after the reflection beam outlet of the present device.

Acknowledgements

We would like to thank Professors H. Sugawara, M. Furusaka, Y. Endoh, H. Ikeda and N. Watanabe for illuminating discussions.

1) C. F. Majkrzak, V. Nunez, J. R. D. Copley, J. F. Anker and G. C. Greene: *SPIE Proc.* 1738 (1992) 90; J. L. Wood: *SPIE Proc.* 1738 (1992) 22.

2) F. Mezei: *SPIE Proc.* 983 (1989) 10; Th. Krist, C. Pappas, Th. Keller and F. Mezei: *Physica* B 213&214 (1995) 939.

3) for example, S.Itoh, T. Watanebe and Y. Endoh: *Proc. 11th Meeting Int. Collab. Avd. Neutron Sources ICANS-XI, Tsukuba, 1990,* KEK Report 90-25, p. 792.

4) O. Schärpf: *AIP Conf. Proc.* 89 (1982) 182.

5) J. L. Wood (Osmic Inc.): private communication (1995).

6) for example, S. Yamada, T. Ebisawa, N. Achiwa, T. Akiyoshi and S. Okamoto: *Annu. Rep. Res. Reactor Inst. Kyoto Univ.* 11 (1978) 8.

7) *Neutron Cross Sections*, Brookhaven National Laboratory Report BNL 325 (1973).